

Molecular basis for benzimidazole resistance from a novel β -tubulin binding site model

Rodrigo Aguayo-Ortiz^a, Oscar Méndez-Lucio^a, Antonio Romo-Mancillas^a, Rafael Castillo^a, Lilián Yépez-Mulia^b, José L. Medina-Franco^c, Alicia Hernández-Campos^{a,*}

^a Facultad de Química, Departamento de Farmacia, Universidad Nacional Autónoma de México (UNAM), México, DF 04510, Mexico

^b Unidad de Investigación Médica en Enfermedades Infecciosas y Parasitarias, IMSS, México, DF 06720, Mexico

^c Mayo Clinic, 13400 East Shea Boulevard, Scottsdale, AZ 85259, USA

ARTICLE INFO

Article history:

Accepted 31 July 2013

Available online 13 August 2013

Keywords:

β -Tubulin

Benzimidazole-2-carbamate derivatives

Resistance/susceptibility

Homology modeling

Docking

Molecular dynamics

ABSTRACT

Benzimidazole-2-carbamate derivatives (BzCs) are the most commonly used antiparasitic drugs for the treatment of protozoan and helminthic infections. BzCs inhibit the microtubule polymerization mechanism through binding selectively to the β -tubulin subunit in which mutations have been identified that lead to drug resistance. Currently, the lack of crystallographic structures of β -tubulin in parasites has limited the study of the binding site and the analysis of the resistance to BzCs. Recently, our research group has proposed a model to explain the interaction between the BzCs and a binding site in the β -tubulin. Herein, we report the homology models of two susceptible (*Haemonchus contortus* and *Giardia intestinalis*) parasites and one unsusceptible (*Entamoeba histolytica*) generated using the structure of the mammal *Ovis aries*, considered as a low susceptible organism, as a template. Additionally, the mechanism by which the principal single point mutations Phe167Tyr, Glu198Ala and Phe200Tyr could lead to resistance to BzCs is analyzed. Molecular docking and molecular dynamics studies were carried out in order to evaluate the models and the ligand–protein complexes' behaviors. This study represents a first attempt towards understanding, at the molecular level, the structural composition of β -tubulin in all organisms, also suggesting possible resistance mechanisms. Furthermore, these results support the importance of benzimidazole derivative optimization in order to design more potent and selective (less toxic) molecules for the treatment of parasitic diseases.

© 2013 Elsevier Inc. All rights reserved.

1. Introduction

Parasitic diseases caused by protozoa and helminths represent a global health issue that affects humans and animals. For this reason, various sanitary and biological control strategies have been established to counteract the harmful effects of parasites; however, chemotherapy remains an essential tool for combating these infections. 1*H*-Benzimidazol-2-ylcarbamate (carbendazim, CBZ) derivatives, also referred to as benzimidazole-2-carbamate derivatives (BzCs), are among the most widely used antiparasitic drugs for the treatment of nematode infections (nematodiasis) [1–3]. The most commonly used BzCs are the 5(6)-substituted benzimidazole-2-carbamates, which include drugs such as albendazole (ABZ), fenbendazole (FBZ), mebendazole (MBZ), nocodazole (NZ), oxibendazole (OBZ), parbendazole (PBZ), luxabendazole (LBZ) and the sulfoxide metabolites of ABZ (ABZSO, ricobendazole) and FBZ (FBZSO, oxfendazole) [4].

Nematodiasis is one of the most widespread parasitic diseases, infecting more than a half of the world's population, mainly presenting itself as gastrointestinal and systemic infections. The gastrointestinal infections in humans are mainly caused by *Ascaris* spp. (ascariasis), *Trichuris trichiura* (trichuriasis), *Ancylostoma duodenale* (ancylostomiasis), *Necator americanus* (necatoriasis) and *Trichinella spiralis* (trichinellosis), whereas in animals, *Haemonchus contortus* (haemonchosis) and *Teladorsagia circumcincta* (teladorsiasis) are the main causes. Additionally, systemic infections are caused by *Wuchereria bancrofti* and *Brugia malayi* (filariasis). Currently, these nematode infections have been treated with the BzCs [5–7]. The BzCs have also shown activity against some protozoan parasites such as *Giardia intestinalis* (giardiasis) and *Trichomonas vaginalis* (trichomoniasis), but not against *Entamoeba histolytica*, *Trypanosoma* spp., *Leishmania* spp. and *Acanthamoeba polyphaga*, in which they exhibit low or no efficacy [8].

Although BzCs have shown broad spectrum and efficacy, the intensive and inadequate use of these antiparasitic drugs has contributed to the development of resistance. Experimental reports have identified single amino acid mutations associated with the loss of BzC– β -tubulin affinity as the major causes of drug resistance

* Corresponding author. Tel.: +52 5556225287; fax: +52 55562255329.

E-mail address: hercam@unam.mx (A. Hernández-Campos).

Table 1BzCs resistance mutations in the β -tubulin of some nematodes.

Amino acid number	Amino acid replacement	Nematode	Reference
167	Phe \rightarrow Tyr	<i>Haemonchus contortus</i>	[45]
	Phe \rightarrow Tyr	<i>Teladorsagia circumcincta</i>	
198	Glu \rightarrow Ala	<i>Haemonchus contortus</i>	[12,47,60]
200	Phe \rightarrow Tyr	<i>Trichuris trichiura</i>	[56,61]
	Phe \rightarrow Tyr	<i>Haemonchus contortus</i>	[48]
	Phe \rightarrow Tyr	<i>Teladorsagia circumcincta</i>	[13,62]
	Phe \rightarrow Tyr	<i>Trichostrongylus axei</i>	[63]
	Phe \rightarrow Tyr	<i>Trichostrongylus colubriformis</i>	[64]
	Phe \rightarrow Tyr	<i>Wuchereria bancrofti</i>	[65]

[2]. Since the appearance of benzimidazoles as anthelmintic drugs, the incidence of parasitic resistance has increased, particularly in nematodes (e.g., *H. contortus*) [9,10].

It is known that different parasite tubulin isoforms may present high or low affinity for benzimidazoles. Nematodes, cestodes, fungi and protozoa exhibit mostly high affinity isoforms and display a binding site located at the terminal amino group of the monomer of β -tubulin. Resistance occurs when genes encoding for β -tubulin suffer a mutation in their sequence, which causes the loss of affinity for benzimidazoles [11]. Table 1 lists the main mutations associated with resistance in nematodes as a result of a single nucleotide transversion in the DNA strand at codons 167, 198 and 200 [10,12–14]. In a similar way, mutations at codons 6, 50, 134, 165, 167, 198, 200 and 240, have been associated with resistance to BzCs in some fungi [15–18].

For the protozoa parasites, these mutations have not shown to be directly related to susceptibility or resistance to these drugs. For example, Upcroft and coworkers studied a benzimidazole resistant strain of *Giardia duodenalis*, but no mutations in the gene sequence coding for the β -tubulin were found. These results suggest that this parasite may have another mechanism of resistance to BzCs [19]. On the other hand, similar studies carried out on the β -tubulin of *Vittaforma corneae* suggest that the resistance of this intracellular protozoan may be due to the presence of a glutamine at position 198 instead of a glutamic acid residue presented in susceptible organism sequences [20].

Unlike mammalian tubulin, there has not been experimental resolution of a crystallographic structure corresponding to helminths or protozoa β -tubulin, hindering the study of this protein. Recently, our research group has proposed a homology model of a parasite β -tubulin, highlighting a binding site that includes the most common amino acid mutations associated with drug resistance (Phe167Tyr, Glu198Ala and Phe200Tyr) and the binding mode of BzCs in it. This model serves as a valuable tool to explain the causes of susceptibility and resistance across different organisms [21].

In this paper several homology models of different nematodes, protozoa and mammalian β -tubulins were reported in order to gain a deeper insight into the action of BzCs in susceptible and unsusceptible organisms. Additionally, the mutations at positions 167, 198 and 200 in the *H. contortus* β -tubulin isotype-1 were evaluated to explain the resistance produced when these mutations occur. Molecular docking and molecular dynamics simulations were also carried out to analyze the different models and to determine the role of certain amino acids in the resistance or susceptibility of β -tubulin towards BzCs.

2. Materials and methods

2.1. Sequence alignment and phylogenetic analysis

Amino acid sequences corresponding to the β -tubulin of different mammals, nematodes and protozoa were retrieved from the

NCBI-Protein database [22]. In a second step, sequences were submitted to the Phylogeny.fr platform [23] for a sequence analysis using MUSCLE (v3.7) [24] and for the integration of the information in a phylogenetic tree using the maximum likelihood method as implemented in PhyML (v3.0 aLRT) [25]. The phylogenetic tree was transformed to a cladogram with TreeDyn (v198.3) [26] and the sequences were grouped together into families to propose relationships between different types of species. Finally, a multiple sequence alignment of the β -tubulins corresponding to eleven unsusceptible/resistant and eleven susceptible organisms was carried out with Clustal O (v1.1.0) [27] to identify structural related positions in the principal residues that constitute the proposed benzimidazole binding site in the β -tubulin.

2.2. Models generation

2.2.1. Homology modeling

In this study, homology models were generated for the β -tubulin of four different organisms which were selected based on their susceptibility to the treatment with BzCs. Three-dimensional models were constructed to corroborate the amino acid differences observed in the sequence alignment and to be used for the molecular modeling studies. The isotype-1 of *H. contortus* and *G. intestinalis* β -tubulins were chosen as the susceptible group, while the unsusceptible group was composed of *E. histolytica* and *O. aries* (low susceptibility [28]) β -tubulin sequences. The homology modeling of these proteins was carried out with MODELLER 9v10 software [29], using residues 1–428 of the β -tubulin sequences and employing the D chain of the *Ovis aries* β -tubulin crystallographic structure (PDB ID: 3N2G) [30] as a template. As some residues in the template three-dimensional structure were missing, the missing side chain atoms were added using the WHAT IF Web Interface (<http://swift.cmbi.ru.nl/servers/html/index.html>). All the final models were evaluated by the QMEAN6 score [31] to obtain an estimation of the local quality of the model, whereas the quality of the protein stereochemistry was assessed using PROCHECK [32]. The models and the corrected template (PDB: 3N2G.D) were subjected to an energy minimization employing the AMBER99SB-ILDN force field [33] and a single point charge water model with a time step of 0.002 ps, using GROMACS 4.5.3 package [34].

2.2.2. Residue replacement models

GenBank-Protein database allowed for the identification of three main BzCs resistant mutations: a phenylalanine to tyrosine mutations at positions 167 (Phe167Tyr) and 200 (Phe200Tyr), and a mutation of a glutamic acid to alanine at the position 198 (Glu198Ala). The final model of *H. contortus* β -tubulin isotype-1 was used to generate the three mutated models employing the residue replacement tool of UCSF Chimera v1.6.1 [35]. The mutated models were subjected to an energy minimization using the same force field and parameters described above.

Table 2

Chemical structures of the BzCs antiparasitic drugs.

Conformations		Compound	R
	<i>cis</i> -1,5	CBZ (carbendazim)	H
	<i>trans</i> -1,5	ABZ (albendazole)	
		(+) ABZSO (ricobendazole)	
		(-) ABZSO (ricobendazole)	
	<i>cis</i> -1,6	OBZ (oxibendazole)	
	<i>trans</i> -1,6	PBZ (parbendazole)	
		LBZ (luxabendazole)	
		MBZ (mebendazole)	
		NZ (nocabendazole)	

2.3. Molecular docking

Molecular docking studies were performed in order to identify any structural difference that might promote or prevent the binding of the BzCs to the proposed binding site in the β -tubulin. These calculations were carried out following the same workflow used to identify the binding site in the β -tubulin [21]. The compounds listed in Table 2 were constructed and submitted to a geometry optimization employing the MMFF94x force field in Spartan'10 [36]. The torsional root and branches of the ligands were chosen using MGLTools 1.5.4 [37], allowing flexibility for all rotatable bonds of the ligand except for the amide bond, which was fixed. In addition, MGLTools 1.5.4 was used to assign Gasteiger–Marsili atomic charges to all ligands [38]. The isomerism of the carbamate group, the inherent tautomerism of the benzimidazole ring system and the enantiomeric behavior of ABZSO were also taken into account. These considerations led to four different groups of isomeric molecules: *cis*-1,5; *trans*-1,5; *cis*-1,6 and *trans*-1,6 (Table 2).

Docking calculations were performed using the AutoDock 4.2 software [39]. A grid box of $80 \times 80 \times 80$ points with a grid spacing of 0.375 \AA and centered at the amino acid 200 was used to calculate the atom types needed for the calculation. The Lamarckian genetic algorithm was used as a search method with a total of 20 runs undertaken with a maximal number of 5,000,000 energy evaluations and initial populations of 150 conformers. The best binding mode of each molecule was selected based on the lowest binding free energy and the largest cluster size.

2.4. Molecular dynamics

Two different studies were performed using molecular dynamics (MD). In the first one, we evaluated the stability of the ligand–protein complexes resulting from the docking of all the compounds in the susceptible and unsusceptible β -tubulin homology models. In this stage, we only used the binding poses that presented the lowest calculated binding free energy of each compound. In the second one, we performed a simulation of the mutated β -tubulin models without a ligand, in order to understand the structural behavior of the resistance mutations.

The MD simulations were prepared following a similar method as in previous publications with an increased simulation time [21,40]. The ligand parameters were calculated with ACPYPE interface [41] in the framework of the AMBER force field. The protein and the complexes were solvated with water in a periodic cubic box that comprised the protein and 1.0 nm of water on all sides. Na^+ and Cl^- atoms were added randomly in order to neutralize the charge of the system and to achieve a concentration of 0.15 M . In a first step, an energy minimization of the systems was carried out employing the AMBER99SB-ILDN force field, a single point charge water model and a time step of 0.002 ps . Electrostatic forces were calculated with the PME implementation of the Ewald summation method [42], and the Lennard-Jones and Coulomb interactions were computed within a cut-off radius of 1.0 nm . Following energy minimization, the system was equilibrated by 20 ps of MD with position restraints on the protein, enabling the relaxation of the solvent molecules. Finally, a 10 ns MD was performed for each of the ligand–protein complexes

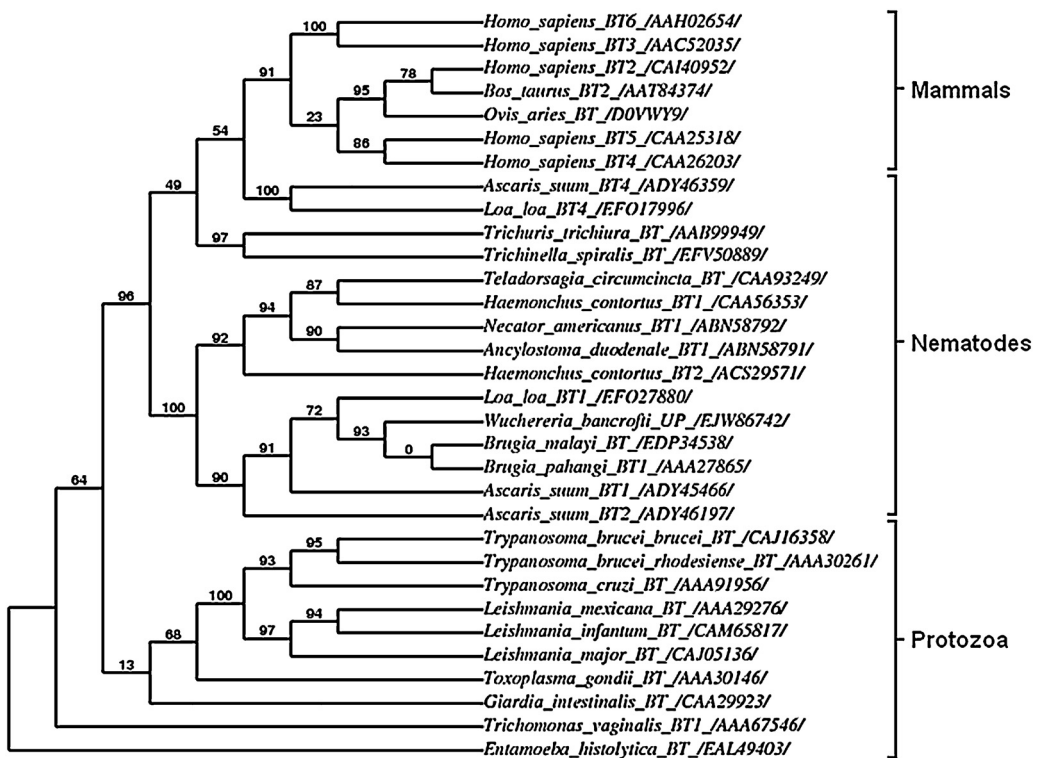


Fig. 1. Strict consensus cladogram based on β -tubulin amino acid sequences from different mammal, nematode and protozoan organisms. The numbers at the nodes indicate values (in percentage) retrieved from the analysis performed using the maximum likelihood method implemented in the PhyML program (v3.0 aLRT). Sequences are represented by the names of the organisms followed by the isotype (BT) and the GenBank accession number of the corresponding β -tubulin. The *O. aries* sequence and accession number was retrieved from the UniProt server [58].

and 30 ns for the mutated β -tubulin models using a time step of 2 ps and 3 ps, respectively. RMSD, hydrogen bonding and binding free energy of the complexes were analyzed during the molecular dynamics study. The calculation of the binding free energy was based on the linear interaction energy (LIE) method equation [43]. All the MD simulations were carried out at 1 bar and 300 K using GROMACS 4.5.3 software.

3. Results and discussion

3.1. Sequence alignment and phylogenetic analysis

The phylogenetic analysis of mammal, nematode and protozoan β -tubulins revealed a relationship between the organisms based on the amino acid sequence similarity of this protein. A previous study carried out with a larger number of tubulin sequences, showed that β -tubulin family is more similar to each other than other families of tubulins [44]. The cladogram represented in Fig. 1 shows the different isotypes of the amino acid sequences (BT) and the accession numbers to the GenBank-Protein database (presented between slashes). As can be observed, the cladogram reveals a clear division between the family classes of organisms in which some of the nematode β -tubulin sequences exhibit high similarity to mammalian ones (more than 90% of identity), seen in *Ascaris suum* isotype 4 (GenBank: ADY46359), *Loa loa* isotype 4 (GenBank: EFO17996), *Trichuris trichiura* (GenBank: AAB99949) and *T. spiralis* (GenBank: EFV50889). On the other hand, evolutionary distance between protozoa and mammalian β -tubulins is greater due to an increase in amino acid sequence differences; however, *G. intestinalis* (GenBank: CAA29923) and *Toxoplasma gondii* (GenBank: AAA30146) are closer to the mammalian branching nodes, having an identity over 80% with most of the mammalian β -tubulin sequences.

A multiple alignment of different β -tubulin sequences was performed using Clustal O in order to correlate the amino acid similarity of the sequences with the phylogenetic analysis. Subsequently, with this alignment, two groups were formed with eleven organisms in each, selected based on their susceptibility (S) and low susceptibility or resistance (R) to the treatment with BzCs [5,8]. Fig. 2 shows the partial sequence alignment of both groups, highlighting the principal residues in the binding site region. These residues could help explain the differences in affinity of BzCs to the β -tubulin of both groups, mainly considering those amino acids associated with resistance mutations in different β -tubulin isotypes of *H. contortus* (e.g., Phe167 [45,46], Glu198 [12,47], and Phe200 [48]). Based on the alignment, it was possible to confirm that the main differences in amino acid sequences are presented at positions 165, 167, 198 and 200. It is worth noting that sequences in the majority of organisms susceptible to BzCs present a high conservation of phenylalanine and that the change to a tyrosine reduces the affinity of BzCs to β -tubulin (e.g., *H. contortus* β -tubulin). The changes of phenylalanine for a tyrosine, methionine or glutamine were seen to present themselves at position 200 in unsusceptible and resistant organisms. Also, the position 167, very similar to 200, exhibits a high conservation of the amino acid phenylalanine in the susceptible group and the change to tyrosine has been observed in some resistant organisms. The hydroxyl group on the tyrosine allows it to function as a hydrogen bond donor/acceptor and increases the polarity and hydrophilicity of the binding site, characteristic unseen with the nonpolar and hydrophobic phenylalanine. However, the presence of this tyrosine at position 167 in the sequence of *T. vaginalis* (susceptible protozoan) suggests that this change may not be relevant in all β -tubulins. This could be an indication that amino acids at position 198 might play a major role in the binding of BzCs to β -tubulin (e.g., differences presented between the protozoa *T. vaginalis* and *E. histolytica*). Finally, the



Fig. 2. Alignment of partial β -tubulin sequences from benzimidazole susceptible (S) and unsusceptible or resistant (R) organisms. The most important residues in the binding site region are represented in boxes, with corresponding residue number. Sequences were obtained from the GenBank database. Mutated sequences (MT) of the *H. contortus* β -tubulin isotype-1: Phe167Tyr (GenBank: AFI57265), Glu198Ala (GenBank: ACS29569), and Phe200Tyr (GenBank: ABM92348); mutated sequence of the *H. contortus* β -tubulin isotype-2: Glu198Ala (GenBank: ACS29573). The MT167 sequence of *H. contortus* was completed using the WT sequence. Sequence alignments were generated using the Jalview 2.8 program [59].

1	MREIVHVQACQCCGNQIGSKFUEVISEDHEGIPQDPGYKGESELQLERINVVYNEAHGGKYV	60	H._contortus_BT1 /CAA56353/
1	MREIVHIQAGQCCGNQIGAKFWEVISDEHGVDPSGEYRGDSLQLERINVVYNEAACGRYYV	60	G._intestinalis /CAA29923/
1	MREISLQIQCQCGNQVGKEFUDLSIQEHHGLSSDGVFGQN-KLQQQLRNVFNFESSTKRUV	59	E._histolytica /EAL49403/
1	MREIVHIQAGQCCGNQIGAKFWEVISDEHGIDPTGSYHGDSDLQLERINVVYNEATGMKVY	60	O._aries_(3N2G:D)
61	***** : * *****: * : * : * : * : * : * : * : * : * : * : * : * : * : * :	120	H._contortus_BT1 /CAA56353/
61	PRAVLVDLEPGTMDSVRSGCPYCQLFRPDNYVFGQSGACGNNAWAKGHYTEGAELVDNULDVV	120	G._intestinalis /CAA29923/
60	PRAILVDLEPGTMDSVRAGPFQCIIFRPDNFVFGQSGAGNNNAWAKGHYTEGAELVDNULDVV	119	E._histolytica /EAL49403/
61	PRSVNVDLEPGTLDALKVKGWHLKFPKDSIIFGNGNAGCAGNNWCKGHYSEGSCLCKMENV	120	O._aries_(3N2G:D)
61	PRAILVDLEPGTMDSVRSGCPQCIIFRPDNFVFGQSGAGNNNAWAKGHYTEGAELVDNULDVV	120	H._contortus_BT1 /CAA56353/
121	***** : * : * : * : * : * : * : * : * : * : * : * : * : * : * : * : * : * :	180	G._intestinalis /CAA29923/
121	RKEAECCDCLQGFQLTHSLGGCTGSGMCTLLISKIREEYPDRIMASFSVVVPSPKVSDTVV	180	E._histolytica /EAL49403/
120	RKRSEACDCLQGFQICHSLGGGTAGAGMCTLLISKIREEYPDRIMNTFSVVVPSPKVSDTVV	180	O._aries_(3N2G:D)
121	RKEVEACECLQGFQVTHSLGGCTGSGCGLTLLISKIRKEEYFDKIIISTYSVVVPSPVSETVV	180	H._contortus_BT1 /CAA56353/
121	RESKESCDCLQGFQLTHSLGGCTGSGMCTLLISKIREEYPDRIMNTFSVVVPSPKVSDTVV	180	G._intestinalis /CAA29923/
181	***** : * : * : * : * : * : * : * : * : * : * : * : * : * : * : * : * : * :	240	E._histolytica /EAL49403/
181	EPYNATLSVHQLVVENTDETFCIDNEALYDICFRTLKLTNPTYGDLNHLVSVTMSGVTTCL	240	O._aries_(3N2G:D)
180	EPYNATLSVHQLVVENTDETFCIDNEALYDICFRTLKLTCPTYGDLNHLVSVTMSGVTTCL	240	H._contortus_BT1 /CAA56353/
181	EPYNCVLSIHKLLESSAIIFCFCDNEALYKITSDIMKEPKPSYESNLTLISSVMSGITCSL	240	G._intestinalis /CAA29923/
181	EPYNATLSVHQLVVENTDETYSIDNEALYDICFRTLKLTPPTYGDLNHLVSVTMSGVTTCL	240	E._histolytica /EAL49403/
181	***** : * : * : * : * : * : * : * : * : * : * : * : * : * : * : * : * : * :	240	O._aries_(3N2G:D)
241	RFPGQLNADLRLKLAVMNMVPPFLRHFMPGCFAPLSAKQAQAYRASSTWAELTQQMFDAKMMH	300	H._contortus_BT1 /CAA56353/
241	RFPGQLNADLRLKLAVNLIPLPFLRHFVLCGFPLTSRCSQIYRALTVEPELVSQMFDAKMMH	300	G._intestinalis /CAA29923/
240	RFPGQLNQDLRLKLAVMNMNPYPRFLRHFSSSIAPVSNALSMKYESLNQGEIIQLFEEKKNTL	299	E._histolytica /EAL49403/
241	RFPGQLNADLRLKLAVMNMVPPFLRHFMPGCFAPLSRCSQIYRALTVEPELTTQQMFDSKMMH	300	O._aries_(3N2G:D)
301	***** : * : * : * : * : * : * : * : * : * : * : * : * : * : * : * : * : * :	300	H._contortus_BT1 /CAA56353/
301	AACDPRHGRYLTVAAFMFRGRMSMREUDDQMISVQNKNSSYFVEWIPNNVKTAVCDDIPPRG	360	G._intestinalis /CAA29923/
300	AASDPRHGRYLTAAMAFRGRMSTKEVD EQMLNIQNKNSSYFVEWIPNNMKWSVCDIPPRG	360	E._histolytica /EAL49403/
301	UDFDPPQSKYFTSSCIIRGKVSTHDVVEEQLFRVRKRNPDLFIPWIPPNMMQLAVCDVPPKG	360	O._aries_(3N2G:D)
301	AACDPRHGRYLTVAAFMFRGRMSMKEVD EQMLNVQNKNSSYFVEWIPNNVKTAVCDDIPPRG	360	H._contortus_BT1 /CAA56353/
301	***** : * : * : * : * : * : * : * : * : * : * : * : * : * : * : * : * : * :	360	G._intestinalis /CAA29923/
361	LKMAATFVGNSTAIQELFKRISSEQFTAMFRRKAFLHWYTGECMDMEHTFEAEASNMDLIS	420	E._histolytica /EAL49403/
361	LKMAATFIGNSTCIOELFKRVCQEFSAMFRKAFLHWYTGECMDMEHTFEAEASNMDLVS	420	O._aries_(3N2G:D)
360	LDLSGTLSNSTAISSDMFKRVYKQFVSHLRKKAFIYLTYTEEGMESEFEEAADLIDLVT	419	H._contortus_BT1 /CAA56353/
361	LKMAATFIGNSTAIQELFKRISSEQFTAMFRRKAFLHWYTGECMDMEHTFEAEASNMDLVS	420	G._intestinalis /CAA29923/
361	***** : * : * : * : * : * : * : * : * : * : * : * : * : * : * : * : * : * :	420	E._histolytica /EAL49403/
421	EYQQYQEA 428 H._contortus_BT1 /CAA56353/	420	O._aries_(3N2G:D)
421	EYQQYQEA 428 G._intestinalis /CAA29923/	420	H._contortus_BT1 /CAA56353/
420	EYQQYTYNA 427 E._histolytica /EAL49403/	420	G._intestinalis /CAA29923/
421	EYQQYQDA 428 O._aries_(3N2G:D)	420	E._histolytica /EAL49403/
421	***** : * : * : * : * : * : * : * : * : * : * : * : * : * : * : * : * : * :	420	O._aries_(3N2G:D)

Fig. 3. Multiple sequence alignment of *Haemonchus contortus* BT1, *Giardia intestinalis* and *Entamoeba histolytica* β -tubulins partial sequences with the *Ovis aries* template sequence (PDB ID: 3N2G.D) used for the homology modeling study. Sequences were aligned with Clustal O 1.1.0.

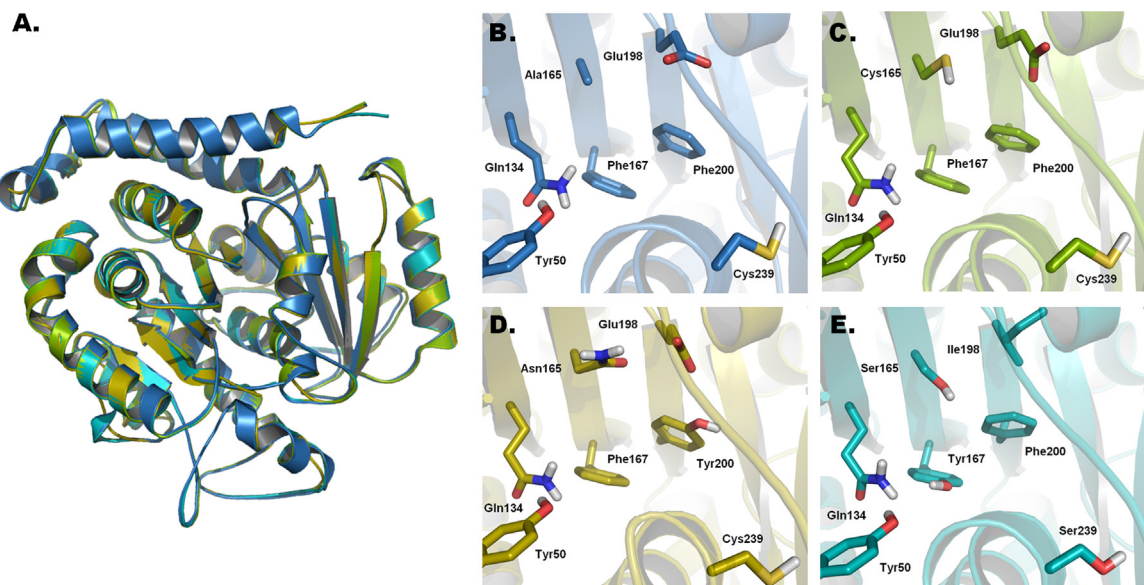


Fig. 4. (A) Superimposed structures of β -tubulin three-dimensional structures, and representation of the principal amino acids that constitute the proposed BzCs binding site on the (B) *H. contortus* BT1, (C) *G. intestinalis*, (D) *O. aries* and (E) *E. histolytica* structures.

differences present at position 165 may only affect the stabilization of the BzCs in the binding site [21].

3.2. Models generation

3.2.1. Homology modeling

Based on the multiple sequence alignment analysis, two unsusceptible (*O. aries* and *E. histolytica*) and two susceptible (*H. contortus* BT1 and *G. intestinalis*) organisms were selected. The three dimensional structures of the β -tubulins of these parasites were modeled using the *O. aries* β -tubulin (PDB ID: 3N2G.D) as a template. Partial sequence alignment of the parasite β -tubulins showed acceptable identity with the template sequence (*H. contortus* BT1 90.7%, *G. intestinalis* 88.0%, and *E. histolytica* 56%) as shown in Fig. 3. Despite the low sequence identity of *E. histolytica* with the template, the three dimensional structure is highly conserved. A similar situation occurs in the β -tubulin sequence of the bacteria *Prosthecobacter dejongeii* (PDB: 2BTQ.B) which shows 36.2% identity with that of *O. aries* while still presenting the same three-dimensional array (superposition and sequence alignment shown in Fig. S1 of the supplementary data).

All the models were built using MODELLER 9v10 software and validated with the PROCHECK server (Figs. S2–S4 of the supplementary data). Ramachandran plot analysis indicates reliability greater than 95.0% for the three models generated. Additionally, these plots

show that all the amino acids comprising the binding site were located in the allowed regions of the plots. Similarly, the Z-score (−1.87 to −1.30) and the QMEANscore (0.61–0.66) showed acceptable values [49] in order to consider all the models suitable for molecular docking studies.

Fig. 4A shows a structural comparison of the modeled β -tubulin of *H. contortus*, *G. intestinalis* and *E. histolytica* with the *O. aries* structure. As it can be observed, there is no significant difference in the tertiary structure of these models. However, important differences were identified in the amino acids present at the binding sites showed in Fig. 4, as observed during the sequence analysis. The binding site pocket of the four structures consists of several highly conserved hydrophobic amino acids (positions 240, 250, 253 and 266) with a few hydrophilic residues (positions 50, 134, 237 and 256), in which the main differences are observed at positions 165, 167, 198 and 200. The different amino acids at these positions could be of great importance to determine the possible cause of susceptibility and resistance to BzCs between organisms.

3.2.2. Residue replacement models

Models of the *H. contortus* β -tubulin isotype-1 containing the mutations Phe167Tyr, Phe200Tyr and Glu198Ala were built in order to find a possible explanation for the mechanisms of resistance in this nematode. Fig. 5 shows the structural differences caused by these mutations, in which the most important

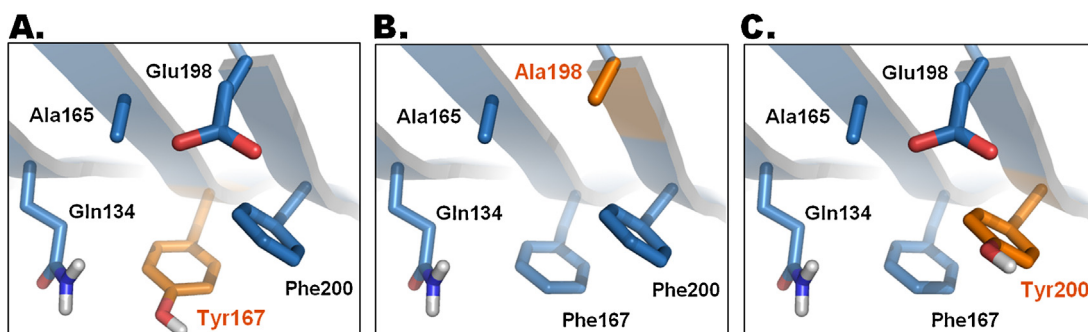


Fig. 5. Three-dimensional representation of the mutated binding sites: (A) Phe167Tyr, (B) Glu198Ala and (C) Phe200Tyr. Mutated amino acids are highlighted and colored in orange.

Table 3Binding free energies and cluster sizes of BzCs in the β -tubulin models.

Compound	Susceptible		Low susceptible		Unsusceptible	
	<i>H. contortus</i> BT1		<i>G. intestinalis</i>		<i>O. aries</i>	
	ΔG_{bind} (kcal/mol)	Cluster size	ΔG_{bind} (kcal/mol)	Cluster size	ΔG_{bind} (kcal/mol)	Cluster size
CBZ	−6.98 ^a	15	−6.92 ^c	16	−7.21 ^{c,*}	20
ABZ	−8.10 ^a	11	−8.18 ^{d,*}	12	−7.54 ^c	16
(+) ABZSO	−8.55 ^a	8	−8.73 ^{d,*}	15	−7.86 ^c	11
(−) ABZSO	−8.54 ^a	11	−8.57 ^{d,*}	14	−7.98 ^d	11
OBZ	−8.17 ^{a,*}	12	−7.63 ^b	13	−7.12 ^c	16
PBZ	−8.09 ^a	11	−8.10 ^{d,*}	14	−7.40 ^d	6
LBZ	−9.46 ^{a,*}	10	−9.25 ^d	2	−8.84 ^d	3
MBZ	−9.43 ^{a,*}	18	−9.08 ^d	10	−8.98 ^c	11
NZ	−9.36 ^{a,*}	19	−9.10 ^d	11	−8.80 ^c	9

^a Conformation *cis*-1,5.^b Conformation *cis*-1,6.^c Conformation *trans*-1,5.^d Conformation *trans*-1,6. For CBZ the letter only refers to the isomerism of the carbamate.

* Lowest energy conformation for each compound in the four organisms. Full details of binding free energies and cluster size for each conformation are reported in Table S1 (supplementary data).

modification is a change in the spatial arrangement of the amino acids. The Phe167Tyr and Phe200Tyr mutations result in an increased polarity in the binding site, which indicates that the electronic factor could be hindering the binding of BzCs. On the other hand, a Glu198Ala mutation shows the loss of a hydrogen bonding acceptor and reduces the length of the aliphatic chain, which causes the formation of an oversized hydrophobic cavity in the binding site.

3.3. Molecular docking

3.3.1. Susceptible and unsusceptible β -tubulin models

The BzCs were docked into a previously proposed binding site [21] using AutoDock 4.2 in order to compare their binding mode in the different β -tubulin models. The lowest calculated binding free energy of the best tautomer and the *cis*, *trans* conformers of each molecule are listed in Table 3 (complete energy results are

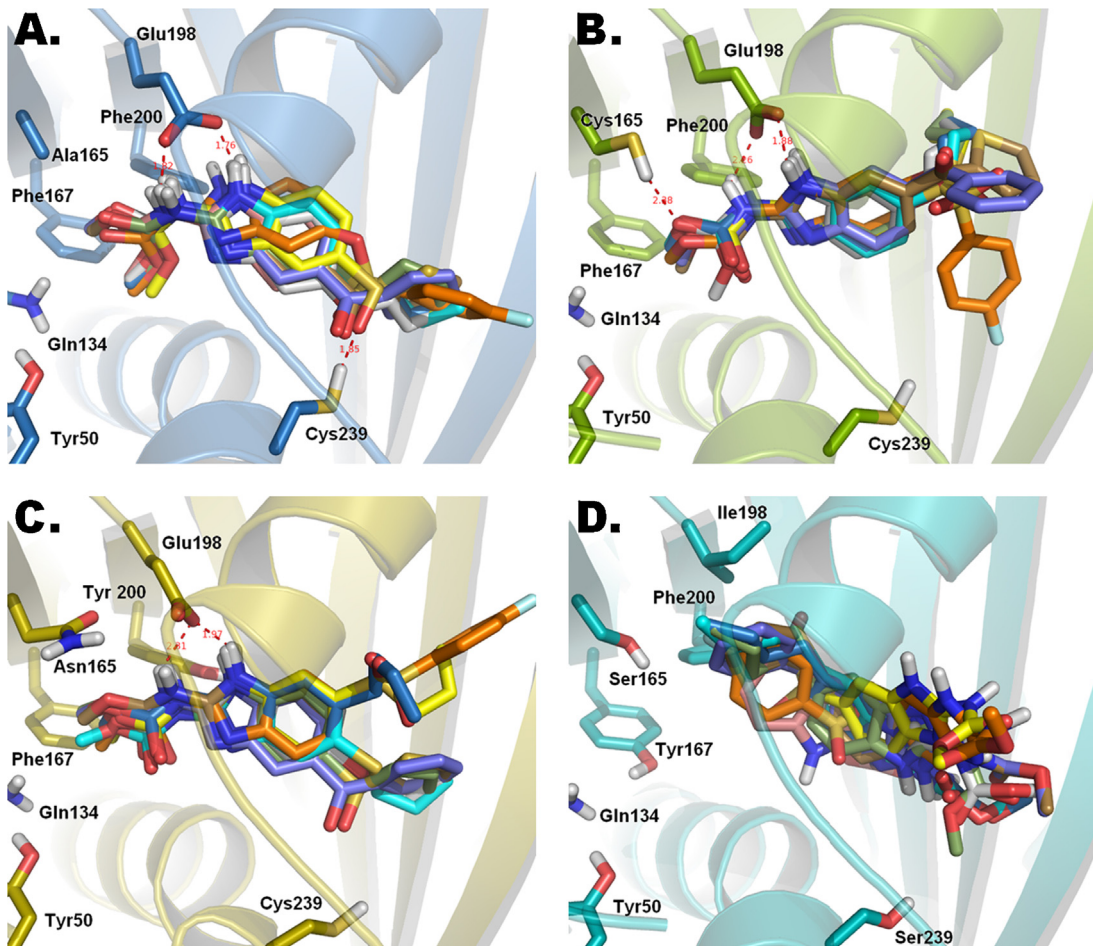


Fig. 6. Predicted binding modes of different BzCs inside the binding site of the (A) *H. contortus*, (B) *G. intestinalis*, (C) *O. aries* and (D) *E. histolytica* β -tubulins. Evaluated ligands: CBZ (pink), ABZ (cyan), (+) ABZSO (green), (−) ABZSO (yellow), OBZ (gray), PBZ (blue), LBZ (orange), MBZ (purple) and NZ (brown). The dotted red lines represent distances, in angstroms, for the formation of hydrogen bonds.

Table 4Binding energies and cluster sizes of BzCs in the wild type (WT) and mutated (MT) models of β -tubulin isotype-1 of *H. contortus*.

Compound	WT		MT					
			Phe167Tyr		Glu198Ala		Phe200Tyr	
	ΔG_{bind} (kcal/mol)	Cluster size						
CBZ	−6.98 ^a	15	−7.02 ^c	19	−6.37 ^c	2	−7.19 ^{c,*}	7
ABZ	−8.10 ^a	11	−8.07 ^a	15	−7.05 ^b	10	−8.22 ^{a,*}	10
(+) ABZSO	−8.55 ^a	8	−8.43 ^a	16	−7.17 ^c	17	−8.78 ^{a,*}	9
(−) ABZSO	−8.54 ^{a,*}	11	−8.37 ^b	2	−7.23 ^b	7	−8.47 ^a	7
OBZ	−8.17 ^a	12	−8.09 ^a	18	−6.66 ^d	15	−8.28 ^{a,*}	17
PBZ	−8.09 ^a	11	−8.15 ^d	12	−7.05 ^b	5	−8.26 ^{a,*}	5
LBZ	−9.46 ^a	10	−9.26 ^a	11	−8.82 ^b	10	−9.62 ^{a,*}	6
MBZ	−9.43 ^c	18	−9.46 ^c	18	−8.26 ^d	8	−9.48 ^{c,*}	16
NZ	−9.36 ^{c,*}	19	−9.35 ^c	15	−7.99 ^a	4	−9.35 ^a	14

^a Conformation *cis*-1,5.^b Conformation *cis*-1,6.^c Conformation *trans*-1,5.^d Conformation *trans*-1,6. For CBZ the letter only refers to the isomerism of the carbamate.

* Lowest energy conformation for each compound in the four organisms. Full details of binding free energies and cluster size for each conformation are reported in Table S2 (supplementary data).

reported in Table S1 of the supplementary data). Fig. 6 shows the proposed binding modes of some of the ligands tested in the four β -tubulin binding sites. In the cases where the BzCs bind to the β -tubulin of a susceptible organism, two different behaviors were observed. In the *H. contortus* binding model, a *cis* conformation in the carbamate and a 1,5 tautomerism in the benzimidazole favor the formation of hydrogen bonds between the Glu198 and the benzimidazole (H-bond distance of 1.7–1.8 Å). Currently, experimental studies confirm the importance of this amino acid in other organisms, such as fungi, in which some groups discussed the idea that the Glu198 might act as the anchor point when a BzC enters the molecular target [50,51]. Moreover, in this model, LBZ, MBZ, NZ, ABZ, ABZSO and OBZ, which present a hydrogen bond acceptor at position 5 of the benzimidazole nucleus, enable the formation of a hydrogen bond with the Cys239 (1.8–2.0 Å). Furthermore, this conformational behavior is very similar to the one reported for *T. spiralis* [21]. Unlike *H. contortus*, in the *G. intestinalis* binding model, a *trans* conformation in the carbamate is favored without losing the interaction with Glu198. The high structural similarity of the binding site in both parasites suggests that the conformational difference is due to the orientation of the Glu198 and Cys239. The absence of the interaction between the substituent in the benzimidazole and the cavity occurs when the Cys239 residue flips out, preventing the hydrogen bond formation. However, it is also noted that the presence of a cysteine at position 165 allows the generation of an additional hydrogen bond interaction between

this residue and the carbamate group (2.0–2.3 Å), stabilizing the molecules inside the binding site.

Interestingly, a hydrogen bond donor at position 165 is also present in unsusceptible models. However, for binding modes of BzCs in *O. aries* β -tubulin, the ligands interact with the Glu198 and not with Asn165. This lack of interaction may result mainly due to the conformation of Asn165 which does not favor the generation of a stable hydrogen bond, unlike serine, threonine or cysteine residues. This could be the reason why there are different binding modes in this model. It is also important to note that the binding energies obtained for *O. aries* are greater than those for the susceptible organisms, but lower than those obtained for *E. histolytica*. Additionally, the interaction with Glu198 allows a similar arrangement of the ligands compared with the susceptible organisms' binding conformations. These results could help in understanding why BzCs have little effect in the mammalian host β -tubulin [28,52,53]. Therefore, it is suggested that the mechanism of resistance mainly arises due to the closure of the binding site preventing drug internalization or the presence of intramolecular interactions which modify the binding modes of the drug.

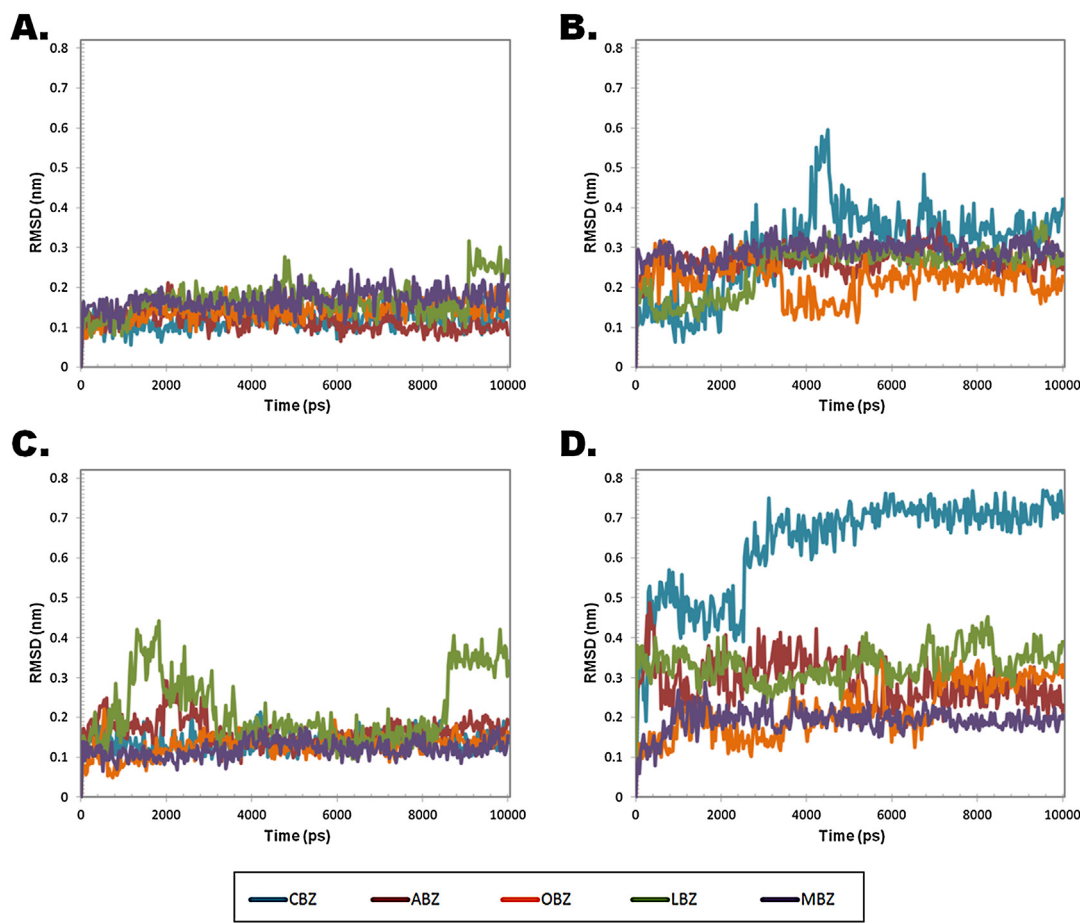
Based on the above results, it is suggested that the affinity of the benzimidazole derivatives for the proposed binding site is mainly due to the formation of hydrogen bonds between Glu198 and two hydrogens in the molecule, one in the benzimidazole and the other in the carbamate group. The importance of the interaction with this residue can be defined in the results obtained with

Table 5

Estimate binding free energies calculated by LIE method and hydrogen bonds of the protein-ligand complexes during molecular dynamics.

Compound	Susceptible				Low susceptible		Unsusceptible	
	<i>H. contortus</i> BT1		<i>G. intestinalis</i>		<i>O. aries</i>		<i>E. histolytica</i>	
	ΔG_{bind} (kJ/mol)	H-bond average						
CBZ	−55.08 ^a	1	−6.89	1	−41.66	2	−17.57	1
ABZ	−68.41	1	−70.55 ^a	2	−55.11	3	−20.15	2
(+) ABZSO	−62.28	2	−16.04	2	−75.49 ^a	2	6.63	1
(−) ABZSO	−65.74 ^a	1	−35.40	2	−37.35	2	47.25	0
OBZ	−67.27 ^a	1	−63.02	2	−51.96	2	−21.80	2
PBZ	−65.59 ^a	2	−42.01	2	−48.11	2	−3.58	1
LBZ	−64.77 ^a	1	−57.19	2	−40.76	2	−10.79	1
MBZ	−60.53	1	−52.93	1	−61.47 ^a	2	14.14	1
NZ	−64.61 ^a	1	−56.63	2	−61.15	2	13.19	1

* Lowest energy for each compound in the four organisms. Full details of estimated binding free energies and hydrogen bonding interactions are reported in Table S3 (supplementary data).



Compound	RMSD (Å)			
	<i>H. contortus</i> BT1	<i>G. intestinalis</i>	<i>O. aries</i>	<i>E. histolytica</i>
CBZ	0.120	0.341	0.141	0.680
ABZ	0.113	0.270	0.160	0.285
(+) ABZSO	0.125	0.258	0.143	0.188
(-) ABZSO	0.178	0.222	0.150	0.233
OBZ	0.148	0.214	0.136	0.232
PBZ	0.111	0.299	0.332	0.318
LBZ	0.178	0.271	0.213	0.330
MBZ	0.175	0.298	0.122	0.195
NZ	0.120	0.291	0.105	0.287

Fig. 7. Ligand positional RMSD of the BzCs inside the binding site of (A) *H. contortus* BT1, (B) *G. intestinalis*, (C) *O. aries* and (D) *E. histolytica* β -tubulins through 10000 ps of simulation with a 10 ps time step. The table summarizes the RMSD average of the last 8 ns of simulation for each organism.

the *E. histolytica* model, where it is clearly observed that there was a decrease in affinity for the binding site due to the loss of this interaction.

Regarding the favored structural conformation of the ligands, it could be said that *cis* and *trans* conformations in the carbamate can be found in similar proportions for the binding interaction, because both allow exposure of a hydrogen bond acceptor group for the interaction with the amino acid 165 if it is possible. For both benzimidazole tautomers, the incidence is associated with the presence or absence of interaction with the amino acid 239. Furthermore, the presence of a carbonyl group or a sulfoxide group at position 5 on the benzimidazole nucleus enables a hydrogen bond with residue 239, as can be seen in LBZ, MBZ, NZ and ABZSO. Curiously, the

ether and thioether groups in the ABZ and OBZ can also form this hydrogen bond; however, the hydrogen bonds formed by these groups usually are not as strong as those formed by a carbonyl or a sulfoxide group, a fact that is reflected in the calculated binding free energy.

3.3.2. Mutated β -tubulin models

Additionally, a molecular docking study of the BzCs into the mutated models of the *H. contortus* β -tubulin isotype-1 (Phe167Tyr, Glu198Ala, and Phe200Tyr) was performed. The binding free energy and cluster size corresponding to the lowest energy conformations of all the BzCs in each model are listed in Table 4. Only the best tautomer and *cis*, *trans* conformer of each molecule

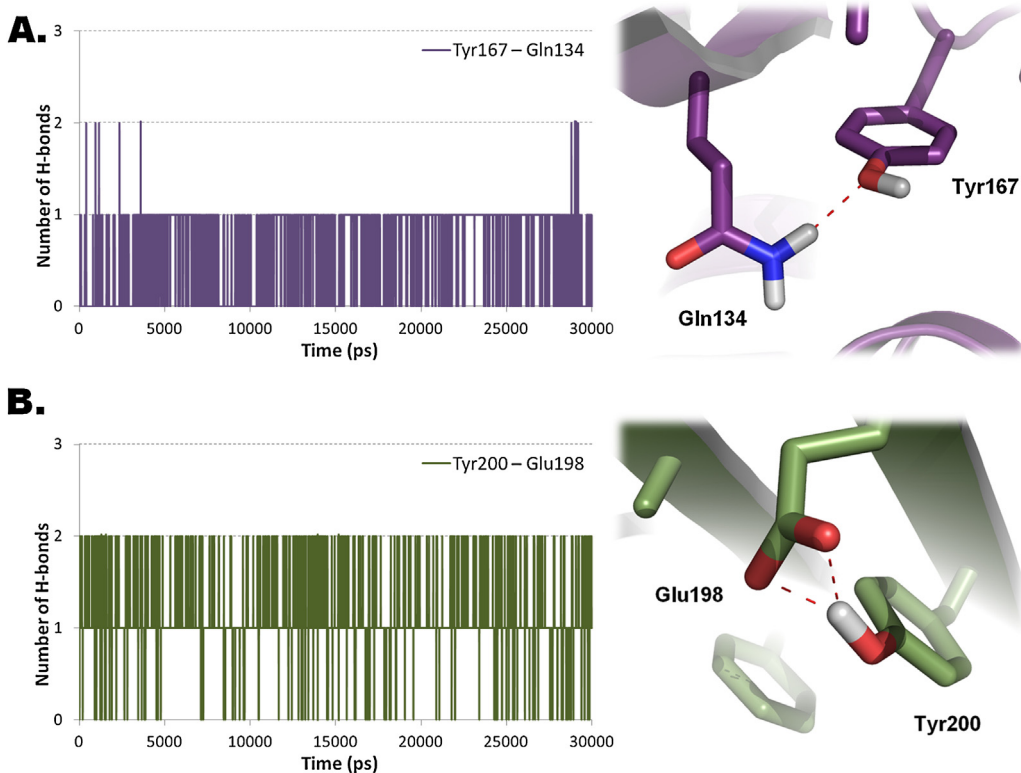


Fig. 8. Time-evolution of hydrogen bonding interactions between the pairs (A) Tyr167–Gln134 and (B) Tyr200–Glu198 through 30 ns of simulation, and schematic representation of the interaction after 20 ns of simulation.

is reported (complete energy results are reported in Table S2 of the supplementary data). A general increase of the binding energy in the model with Glu198Ala mutation was observed as a result of a different arrangement of the BzC in the binding site, similar to the results observed in the *E. histolytica* model. These results highlight, once again, the importance of a glutamate at position 198, since this residue stabilizes the ligand inside the binding site. Similar binding free energies and binding modes were observed for the wild-type model and those with mutations at positions 167 and 200, suggesting that mutations at these positions do not directly affect the ligand–protein interaction. Nevertheless, as proposed for *O. aries*, these mutations could be hindering the internalization of the ligand into the pocket.

3.4. Molecular dynamics studies

3.4.1. Susceptible and unsusceptible β -tubulin models

Molecular dynamics (MD) simulations of ligand–protein complexes were performed in order to compare the binding behavior of each BzC into the four β -tubulins analyzed in this study. In order to establish quantitative insights into the binding affinity of BzCs for the β -tubulin binding site, the number of hydrogen bonds and the binding free energies based on the LIE method of ligand–protein complexes were calculated with GROMACS 4.5.3 (Table S3 of the supplementary data). Average number of hydrogen bonds and the binding free energies for coupling in each organism are reported in Table 5. To assess the stability of the complexes, the root mean square deviations (RMSD) were calculated as a function of the simulation time of each complex. Fig. 7 shows the ligand positional RMSD of the ligand–protein complexes with CBZ, ABZ, OBZ, LBZ and MBZ for each organism; the table beneath the plots shows the RMSD average of the MD simulation of all ligand–protein complexes, discarding the first 2 ns as the equilibration time.

As observed in the molecular docking studies, the BzC– β -tubulin complexes of *H. contortus* presented the lowest binding free energies of the four models, followed by *G. intestinalis* and *O. aries* complexes respectively, which presented similar binding energy values. Additionally, the analysis of these complexes also revealed a high conservation of the hydrogen bonds between the BzCs and Glu198 throughout the simulation. With this, the importance of this interaction to stabilize the BzCs in the β -tubulin binding site is confirmed. Furthermore, the ligand positional RMSD showed that the *H. contortus* and *O. aries* ligand–protein complexes presented the lowest RMSD values, compared with the protozoan models. This was the expected result for the model of *H. contortus* based on the results obtained during the docking; however, the stability of the ligands inside *O. aries* β -tubulin may be due to the interaction with the amino acid Tyr200. Particularly, MBZ and NZ presented low calculated binding energies and the lowest RMSD in *O. aries* β -tubulin during the MD simulations. Furthermore, these compounds are located close to the amino acid Leu240, whose mutation to isoleucine has been identified in tumor cell lines resistant to the treatment with vincristine [54]. These results suggest an explanation of the anticancer behavior of both drugs and the competitive inhibition of colchicine binding to β -tubulin [21,55]. On the other hand, *E. histolytica* BzC– β -tubulin complexes exhibit a more positive binding energy, less stable hydrogen bonds and the highest RMSD values. Once again, these results confirm the highest affinity of BzCs for the susceptible organisms' β -tubulins compared with *E. histolytica*, establishing a correlation between the amino acid composition of the binding site of each model with the resistance and susceptibility. Nevertheless, the similar binding energy and ligand positional RMSD of the ligands in the β -tubulins of *H. contortus* and *G. intestinalis* with *O. aries* suggests that the resistance or low susceptibility of this organism to BzCs is due to another mechanism inherent to the affinity of these for the binding site. A potential mechanism related to the presence of

tyrosine at position 200 of the β -tubulin is proposed in the following section.

3.4.2. Mutated β -tubulin models

The molecular docking study allowed the confirmation of the importance of Glu198 for stabilization of the ligands; it acts by reducing the protein-ligand interaction when alanine mutation occurs. In the case of mutations at phenylalanines 167 and 200, no significant differences in the binding energies were observed. This evidence supports the idea that the mechanism of resistance might be inherent to the coupling of the ligand, and could be intervening during the process of internalization. This proposal is based on the fact that the mutated residue, which has a polar group, acquires the ability to form hydrogen bonds with adjacent amino acids. To probe this hypothesis, the hydrogen bonding of these residues with other amino acids present in the binding site were analyzed, thus evaluating the potential effect of such interactions. Fig. 8 shows the main intramolecular hydrogen bonding interactions observed in the mutated Phe167Tyr and Phe200Tyr β -tubulin models and the percentage of occurrence during 30 ns of MD simulation.

Hydrogen bonding interaction between Tyr167 and Gln134 has low incidence, only present 68.27% of the evaluated time. Nevertheless, it is possible that this interaction might be interfering with the opening process of the binding site, as the Tyr167 and Gln134 are located in two adjacent parallel beta sheets (S4 and S3, respectively). Previously, our research group has proposed that the amino acid Gln134 allows the internalization of the ligand to the binding site; thus, if it is interacting with Tyr167, such internalization would not be favored [21]. It is remarkable that this interaction could explain the low significance of the mutation Phe167Tyr in some organisms, such as *Ascaris lumbricoides* [56]. Nevertheless, more calculations focused on the opening/closing mechanism of the binding site are required to understand the role of this mutation in this process.

On the other hand, the Tyr200 interacts 98.03% of the time with Glu198 during the simulation. Despite the high incidence of this hydrogen bond formation between the hydroxyl group of Tyr200 with the carboxylate group of Glu198, no influence in the binding site opening is expected as these amino acids are located on the same segment of beta sheet (S5). Fig. 8B also shows the orientation change of Glu198 as a result of interaction with Tyr200. The interaction between these amino acids promotes a distancing of Glu198 from its original site, preventing the formation of hydrogen bonds between the Glu198 and other ligands. It is worth noting that most of the resistant organisms present a hydrogen bond donor at position 200 that could be interacting directly with Glu198. A possible interaction between the Tyr200 with the amino acid at position 165 is also considered. Nevertheless, the explanation which considers this interaction cannot be true for all resistant organisms since some of them have a non-polar amino acid at position 165, such as in *H. contortus* BT1 and *T. circumcincta* BT2.

Based on the interaction between Tyr200 with Glu198, it is assumed that the resistance mechanism functions in two different forms: altering the internalization of the ligand into the binding site or reducing the ligand–protein interaction. Moreover, as Glu198–Tyr200 interaction decreases the exposure of Glu198 to the binding site increases the possibility that the ligand interacts initially with the oxygen of the hydroxyl group of Tyr200 instead of interacting directly with Glu198. If the carbamate of the benzimidazole presents a first interaction with the Tyr200, it would lead to an unfavorable coupling and subsequent destabilization of the ligand–protein complex. Nevertheless, this hypothesis suggests that a possibility exists that a favorable interaction occurs eventually, explaining the small effect due to binding in mammalian host β -tubulin.

4. Conclusion

Possible causes of differences in susceptibility to treatment with benzimidazole-2-carbamate derivatives (BzCs) are presented using a new proposed binding site model [21]. This model has proven to be a valuable tool in the study of the differences in affinity and resistance mechanisms to the BzCs. The multiple sequence alignment showed that the main differences in susceptibility are presented at positions 165, 167, 198 and 200 of the β -tubulin sequences. Molecular modeling studies corroborated the binding mode of the BzCs in the β -tubulin binding site and were also in agreement with β -tubulin susceptibility reports based on the treatment with BzCs. The mutated and unsusceptible β -tubulin models suggest that the possible cause of resistance to BzCs is mainly due to amino acid modification at position 198 because of the loss of hydrogen bonding interactions. On the other hand, the substitution of phenylalanine for tyrosine at positions 167 and 200 suggests that the inhibitory mechanism may take place during the opening of the binding site or during the internalization of the ligand. As a result, the benzimidazole-2-carbamate structure must be modified for the improvement of more potent, selective and less toxic molecules for the treatment of parasitic diseases.

Acknowledgements

The authors are very grateful to CONACyT for financial support in project 80093. We thank Anuar Flores-Gahona from Facultad de Química, UNAM, for the English proof of the manuscript and helpful suggestions. We acknowledge DGSCA, UNAM for the support we received in the use of the HP Cluster Platform 4000 Opteron dual core supercomputer (Kan-Balam). R. Aguayo-Ortiz acknowledges the fellowship awarded by Colegio de Profesores and section 024 of AAPAUNAM. He is also grateful to CONACyT for the fellowship granted (No. 510728/288862).

All molecular graphics figures were prepared with PyMOL [57].

Appendix A. Supplementary data

Supplementary data associated with this article can be found, in the online version, at <http://dx.doi.org/10.1016/j.jmgm.2013.07.008>.

References

- [1] C.E. Lanusse, R.K. Prichard, Relationship between pharmacological properties and clinical efficacy of ruminant anthelmintics, *Veterinary Parasitology* 49 (1993) 123–158.
- [2] L. Mottier, C.E. Lanusse, Bases moleculares de la resistencia a fármacos antihelmínticos, *Revista de Medicina Veterinaria* 82 (2001) 74–85.
- [3] D. Márquez Lara, Resistencia a los antihelmínticos: origen, desarrollo y control, *Revista Corpoica* 4 (2003) 55–71.
- [4] S. Sharma, N. Anand, *Approaches to Design and Synthesis of Antiparasitic Drugs*, Vol. 25, Elsevier, Amsterdam, 1997 (Chapter 8).
- [5] B.J. Fennell, J.A. Naughton, J. Barlow, G. Brennan, I. Fairweather, et al., Microtubules as antiparasitic drug targets, *Expert Opinion on Drug Discovery* 3 (2008) 501–518.
- [6] R. Haque, Human Intestinal Parasites, *Journal of Health, Population and Nutrition* 25 (2007) 387–391.
- [7] M.O. Harhay, J. Horton, P.L. Olliaro, Epidemiology and control of human gastrointestinal parasites in children, *Expert Review of Anti-infective Therapy* 8 (2010) 219–234.
- [8] S.K. Katiyar, V.R. Gordon, G.L. McLaughlin, T.D. Edlind, Antiprotozoal activities of benzimidazoles and correlations with β -tubulin sequence, *Antimicrobial Agents and Chemotherapy* 38 (1994) 2086–2090.
- [9] E. Lacey, J.H. Gill, Biochemistry of benzimidazole resistance, *Acta Tropica* 56 (1994) 245–262.
- [10] R.N. Beech, P. Skuce, D.J. Bartley, R.J. Martin, R.K. Prichard, et al., Anthelmintic resistance: markers for resistance or susceptibility? *Parasitology* 138 (2010) 160–174.
- [11] G.W. Lubega, R.K. Prichard, Specific interaction of benzimidazoles anthelmintics with tubulin: high-affinity binding and benzimidazoles resistance in *Haemonchus contortus*, *Molecular and Biochemical Parasitology* 38 (1990) 221–232.

- [12] L. Rufener, R. Kaminsky, P. Mäser, In vitro selection of *Haemonchus contortus* for benzimidazole resistance reveals a mutation at amino acid 198 of β -tubulin, *Molecular and Biochemical Parasitology* 168 (2009) 120–122.
- [13] A. Silvestre, C. Sauve, J. Cortet, J. Cabaret, Contrasting genetic structures of two parasitic nematodes, determined on the basis of neutral microsatellite markers and selected anthelmintic resistance markers, *Molecular Ecology* 18 (2009) 5086–5100.
- [14] G. von Samson-Himmelstjerna, T.K. Walsh, A.A. Donnan, S. Carrière, F. Jackson, et al., Molecular detection of benzimidazole resistance in *Haemonchus contortus* using real-time PCR and pyrosequencing, *Parasitology* 136 (2009) 349–358.
- [15] A.B. Bennett, T.J.C. Anderson, G.C. Barker, E. Michael, D.A.P. Bundy, Sequence variation in the *Trichuris trichiura* β -tubulin locus: implications for the development of benzimidazole resistance, *International Journal for Parasitology* 32 (2002) 1519–1528.
- [16] M.W. Robinson, N. McFerran, A. Trudgett, L. Hoey, I. Fairweather, A possible model of benzimidazole binding to β -tubulin disclosed by invoking an inter-domain movement, *Journal of Molecular Graphics and Modelling* 23 (2004) 275–284.
- [17] Z. Ma, M. Yoshimura, B. Holtz, T. Michailides, Characterization, PCR-based detection of benzimidazole-resistant isolates of *Monilinia laxa* in California, *Pest Management Science* 61 (2005) 449–457.
- [18] B.S. Jarullah, R.B. Subramanian, S. Kajal, J.S. Jarullah, Comparative in-silico study of β -tubulin proteins from *Arthrobotrys musiformis* for resistance to benzimidazole, *International Journal of Bioscience, Biochemistry and Bioinformatics* 2 (2012) 131–135.
- [19] J. Upcroft, R. Mitchell, N. Chen, P. Upcroft, Albendazole resistance in *Giardia* is correlated with cytoskeletal changes but not with a mutation at amino acid 200 in beta-tubulin, *Microbial Drug Resistance* 2 (1996) 303–308.
- [20] C. Franzen, B. Salzberger, Analysis of the β -tubulin gene from *Vittaforma cornea* suggests benzimidazole resistance, *Antimicrobial Agents and Chemotherapy* 52 (2007) 790–793.
- [21] R. Aguayo-Ortiz, O. Méndez-Lucio, J.L. Medina-Franco, R. Castillo, L. Yépez-Mulia, et al., Towards the identification of the binding site of benzimidazoles to β -tubulin of *Trichinella spiralis*: insights from computational and experimental data, *Journal of Molecular Graphics and Modelling* 41 (2013) 12–19.
- [22] S.F. Altschul, T.L. Madden, A.A. Schäffer, J. Zhang, Z. Zhang, et al., Gapped BLAST and PSI-BLAST: a new generation of protein database search programs, *Nucleic Acids Research* 25 (1997) 3389–3402.
- [23] A. Dereeper, V. Guignon, G. Blanc, S. Audic, S. Buffet, et al., Phylogeny.fr: robust phylogenetic analysis for the non-specialist, *Nucleic Acids Research* 36 (2008) W465–W469.
- [24] R.C. Edgar, MUSCLE: multiple sequence alignment with high accuracy and high throughput, *Nucleic Acids Research* 32 (2004) 1792–1797.
- [25] S. Guindon, J.-F. Dufayard, V. Lefort, M. Anisimova, W. Hordijk, et al., New algorithms and methods to estimate maximum-likelihood phylogenies: assessing the performance of PhyML 3.0, *Systematic Biology* 59 (2010) 307–321.
- [26] F. Chevenet, C. Brun, A.-L. Bañuls, B. Jacq, R. Christen, TreeDyn: towards dynamic graphics and annotations for analyses of trees, *BMC Bioinformatics* 7 (2006) 439.
- [27] F. Sievers, A. Wilm, D. Dineen, T.J. Gibson, K. Karplus, et al., Fast, scalable generation of high-quality protein multiple sequence alignments using Clustal Omega, *Molecular Systems Biology* 7 (2011) 539.
- [28] P.A. Friedman, E.G. Platzer, Interaction of anthelmintic benzimidazole derivatives with bovine brain tubulin, *Biochimica et Biophysica Acta* 544 (1978) 605–614.
- [29] A. Fiser, R.K. Do, A. Sali, Modeling of loops in protein structures, *Protein Science* 9 (2000) 1753–1773.
- [30] P. Barbier, A. Dorléans, F. Devred, L. Sanz, D. Allegro, et al., Stathmin and interfacial microtubule inhibitors recognize a naturally curved conformation of tubulin dimers, *Journal of Biological Chemistry* 285 (2010) 31672–31681.
- [31] P. Benkert, M. Künzli, T. Schwede, QMEAN server for protein model quality estimation, *Nucleic Acids Research* 37 (2009) W510–W514.
- [32] R.A. Laskowski, M.W. MacArthur, D.S. Moss, J.M. Thornton, PROCHECK. A program to check the stereochemical quality of protein structures, *Journal of Applied Crystallography* 26 (1993) 283–291.
- [33] K. Lindorff-Larsen, S. Piana, K. Palmo, P. Maragakis, J.L. Klepeis, et al., Improved side-chain torsion potentials for the Amber ff99SB protein force field, *Proteins* 78 (2010) 1950–1958.
- [34] D. Van Der Spoel, E. Lindahl, B. Hess, G. Groenhof, A.E. Mark, et al., GROMACS: fast, flexible, and free, *Journal of Computational Chemistry* 26 (2005) 1701–1718.
- [35] E.F. Pettersen, T.D. Goddard, C.C. Huang, G.S. Couch, D.M. Greenblatt, et al., UCSF Chimera – a visualization system for exploratory research and analysis, *Journal of Computational Chemistry* 25 (2004) 1605–1612.
- [36] Y. Shao, L.F. Molnar, Y. Jung, J. Kussmann, C. Ochsenfeld, et al., Advances in methods and algorithms in a modern quantum chemistry program package, *Physical Chemistry Chemical Physics* 8 (2006) 3172–3191.
- [37] M.F. Sanner, Python: a programming language for software integration and development, *Journal of Molecular Graphics and Modelling* 17 (1999) 57–61.
- [38] J. Gasteiger, M. Marsili, A new model for calculating atomic charges in molecules, *Tetrahedron Letters* 19 (1978) 3181–3184.
- [39] G.M. Morris, R. Huey, W. Lindstrom, M.F. Sanner, R.K. Belew, et al., AutoDock4 and AutoDockTools4: automated docking with selective receptor flexibility, *Journal of Computational Chemistry* 30 (2009) 2785–2791.
- [40] C.A. Méndez-Cuesta, O. Méndez-Lucio, R. Castillo, Homology modeling, docking and molecular dynamics of the *Leishmania mexicana* arginase: a description of the catalytic site useful for drug design, *Journal of Molecular Graphics and Modelling* 38 (2012) 50–59.
- [41] A.W. Sousa da Silva, W.F. Vranken, ACPYPE – AnteChamber PYthon Parser interface, *BMC Research Notes* 5 (2012) 367.
- [42] T. Darden, D. York, L. Pedersen, Particle mesh Ewald: an $N\log(N)$ method for Ewald sums in large systems, *Journal of Chemical Physics* 98 (1993) 10089.
- [43] J. Aqvist, C. Medina, J.E. Samuelsson, A new method for predicting binding affinity in computer-aided drug design, *Protein Engineering* 7 (1994) 385–391.
- [44] J.A. Tuszyński, E.J. Carpenter, J.T. Huzil, W. Malinski, T. Luchko, et al., The evolution of the structure of tubulin and its potential consequences for the role and function of microtubules in cells and embryos, *International Journal of Developmental Biology* 50 (2006) 341–358.
- [45] A. Silvestre, J. Cabaret, Mutation in position 167 of isotype 1 β -tubulin gene of Trichostrongylid nematodes: role in benzimidazole resistance? *Molecular and Biochemical Parasitology* 120 (2002) 297–300.
- [46] H.R. Shokrani, P. Shayan, A. Eslami, R. Nabavi, Benzimidazole-resistance in *Haemonchus contortus*: new PCR-RFLP method for the detection of point mutation at Codon 167 of Isotype 1 β -tubulin gene, *Iranian Journal of Parasitology* 7 (2012) 41–48.
- [47] A.C. Kotze, K. Cowling, N.H. Bagnall, B.M. Hines, A.P. Ruffell, et al., Relative level of thiabendazole resistance associated with the E198A and F200Y SNPs in larvae of a multi-drug resistant isolate of *Haemonchus contortus*, *International Journal for Parasitology: Drugs and Drug Resistance* 2 (2012) 92–97.
- [48] M.S.G. Kwa, J.G. Veenstra, M.H. Roos, Benzimidazole resistance in *Haemonchus contortus* is correlated with a conserved mutation at amino acid 200 in β -tubulin isotype 1, *Molecular and Biochemical Parasitology* 63 (1994) 299–303.
- [49] P. Benkert, M. Biasini, T. Schwede, Toward the estimation of the absolute quality of individual protein structure models, *Bioinformatics* 27 (2010) 343–350.
- [50] J. Qiu, J. Xu, J. Yu, C. Bi, C. Chen, et al., Localisation of the benzimidazole fungicide binding site of *Gibberella zeae* β 2-tubulin studied by site-directed mutagenesis, *Pest Management Science* 67 (2011) 191–198.
- [51] J. Qiu, T. Huang, J. Xu, C. Bi, C. Chen, et al., β -Tubulins in *Gibberella zeae*: their characterization and contribution to carbendazim resistance, *Pest Management Science* 68 (2012) 1191–1198.
- [52] A. Jiménez-González, C. De Armas-Serra, A. Criado-Fornelio, N. Casado Escribano, F. Rodríguez-Caabeiro, et al., Preliminary characterization and interaction of tubulin from *Trichinella spiralis* larvae with benzimidazole derivatives, *Veterinary Parasitology* 39 (1991) 89–99.
- [53] G.J. Russell, J.H. Gill, E. Lacey, Binding of [3 H]benzimidazole carbamates to mammalian brain tubulin and the mechanism of selective toxicity of the benzimidazole anthelmintics, *Biochemical Pharmacology* 43 (1992) 1095–1100.
- [54] J.T. Huzil, K. Chen, L. Kurgan, J.A. Tuszyński, The roles of β -tubulin mutations and isotype expression in acquired drug resistance, *Cancer Informatics* 3 (2007) 159–181.
- [55] T.L. Nguyen, C. McGrath, A.R. Hermone, J.C. Burnett, D.W. Zaharevitz, et al., A common pharmacophore for a diverse set of colchicine site inhibitors using a structure-based approach, *Journal of Medicinal Chemistry* 48 (2005) 6107–6116.
- [56] A. Diawara, C.M. Halpenny, T.S. Churcher, C. Mwandawiro, J. Kihara, et al., Association between response to albendazole treatment and β -tubulin genotype frequencies in soil-transmitted helminths, *PLoS Neglected Tropical Diseases* 7 (2013) e2247.
- [57] W.L. DeLano, The PyMOL Molecular Graphics System, DeLano Scientific LLC, Palo Alto, CA, 2007 <http://www.pymol.org>.
- [58] M. Magrane, U. Consortium, UniProt Knowledgebase: a hub of integrated protein data, *Database (Oxford)* 2011 (2011) bar009.
- [59] A.M. Waterhouse, J.B. Procter, D.M.A. Martin, M. Clamp, G.J. Barton, Jalview Version 2 – a multiple sequence alignment editor and analysis workbench, *Bioinformatics* 25 (2009) 1189–1191.
- [60] M. Ghisi, R. Kaminsky, P. Mäser, Phenotyping and genotyping of *Haemonchus contortus* isolates reveals a new putative candidate mutation for benzimidazole resistance in nematodes, *Veterinary Parasitology* 144 (2007) 313–320.
- [61] A. Diawara, L.J. Drake, R.R. Swiswillo, J. Kihara, D.A.P. Bundy, et al., Assays to detect β -tubulin codon 200 polymorphism in *Trichuris trichiura* and *Ascaris lumbricoides*, *PLoS Neglected Tropical Diseases* 3 (2009) e397.
- [62] P. Shayan, A. Eslami, H. Borji, Innovative restriction site created PCR-RFLP for detection of benzimidazole resistance in *Teladorsagia circumcincta*, *Parasitology Research* 100 (2007) 1063–1068.
- [63] C. Palcy, A. Silvestre, C. Sauve, J. Cortet, J. Cabaret, Benzimidazole resistance in *Trichostrongylus axei* in sheep: long-term monitoring of affected sheep and genotypic evaluation of the parasite, *The Veterinary Journal* 183 (2010) 68–74.
- [64] M.H. Roos, M.S.G. Kwa, W.N. Grant, New genetic and practical implications of selection for anthelmintic resistance in parasitic nematodes, *Parasitology Today* 11 (1995) 148–150.
- [65] A.E. Schwab, D.A. Boakye, D. Kyewele, R.K. Prichard, Detection of benzimidazole resistance-associated mutations in the filarial nematode *Wuchereria bancrofti* and evidence for selection by albendazole and ivermectin combination treatment, *American Journal of Tropical Medicine and Hygiene* 73 (2005) 234–238.